

A Three-Dimensional Finite Element Model for Biomechanical Analysis of the Hip

Guang-Xing Chen · Liu Yang · Kai Li ·
Rui He · Bin Yang · Yan Zhan · Zhi-Jun Wang ·
Bing-Nin Yu · Zhe Jian

Published online: 17 March 2013
© Springer Science+Business Media New York 2013

Abstract The objective of this study was to construct a three-dimensional (3D) finite element model of the hip. The images of the hip were obtained from Chinese visible human dataset. The hip model includes acetabular bone, cartilage, labrum, and bone. The cartilage of femoral head was constructed using the AutoCAD and Solidworks software. The hip model was imported into ABAQUS analysis system. The contact surface of the hip joint was meshed. To verify the model, the single leg peak force was loaded, and contact area of the cartilage and labrum of the hip and pressure distribution in these structures were observed. The constructed 3D hip model reflected the real hip anatomy. Further, this model reflected biomechanical behavior similar to previous studies. In conclusion, this 3D finite element hip model avoids the disadvantages of other construction methods, such as imprecision of cartilage construction and the absence of labrum. Further, it provides basic data critical for accurately modeling normal and abnormal loads, and the effects of abnormal loads on the hip.

Keywords Hip · 3D finite element · Visible human dataset · Biomechanics · Model

Introduction

The complex anatomic structure of the human hip significantly limits biomechanical studies of this joint. Such studies would be beneficial for complex evaluations, assessments of the difficulty of experimental studies, or estimating the need of implants [1–6]. The finite element method, capable of performing high-fidelity simulation and accurate analysis of complex structure of human organs, is currently the most widely applied method for biomechanical analysis [7–9]. Its accuracy depends on precise construction of the anatomic structure. Unfortunately, in the current state, both magnetic resonance imaging (MRI) and computed tomography (CT) imaging of the hip cannot provide the required accuracy in imaging the acetabular cartilage and labrum thus impeding creation of complete and accurate three-dimensional (3D) finite element hip model. Currently, such model can only be built through covering the acetabulum and femoral head bone with a cartilage of arbitrarily defined thickness [9]. Further, precise construction of the labrum model is also challenging [10]. It is still challenging to accurately construct the labrum using the traditional entity cutting construction method, since this method is very complex, requires a large amount of work, and is impeded by a low imaging resolution. By contrast, the newly built Chinese visible human (CVH) dataset [11] may be able to provide traverse images of higher accuracy and larger resolution to enable construction of 3D finite element joint models, also for the hip joint. In the present study, we created models of acetabular bone, cartilage, and labrum, and performed the finite element mechanical analysis and verification.

G.-X. Chen · L. Yang (✉) · R. He · B. Yang · Y. Zhan
Center for Joint Surgery, Southwest Hospital, Gaotanyan Street
30, Shapingba District, Chongqing 400038, China
e-mail: cgx7676@hotmail.com

K. Li
Department of Anatomy, College of Medicine, Third Military
Medical University, Chongqing 400038, China

Z.-J. Wang · B.-N. Yu · Z. Jian
College of Civil Engineering, Chongqing University,
Chongqing 400030, China

Materials and Methods

Instruments, Software, and Environment

We utilized high-performance graphics workstation and 1,000 M local networks capable of parallel computing. Configurations of the server and graphics workstation were as follows: AS-PE1800 server (Intel processor 3.2 GHz, 1 GB ECC memory, 146 GB double disk), AW-670n Graphics Workstation (Intel processor 3.2 GHz, 2 GB memory, 300 GB double disk, 256 M FX3450 graphics card, Dell Tm 20 inch monitor), AutoCAD 2004 (Autodesk, USA), and SolidWorks 2008SP0.0 (SolidWorks, USA). The infinite element analysis software was ABAQUS 6.7 (Simulia, USA).

Image Acquisition

The images employed in this study were obtained from the 5th CVH dataset (CVH5) provided by the Third Military Medical University (TMMU). The utilized datasets ranged from No. CVH513400 to No. CVH514560, with image pixels of $10,000 \times 6,654$ and layer spacing of 0.2 mm. Anatomical regions included the pelvis, hip joint, and the proximal end of the femur. In total, 1,161 images were utilized; of these, 152 images, including the images from the hip, part of acetabulum, upper pelvis, and the proximal end of the femur, were obtained at 0.4-mm sections.

Construction of 3D Models Through Reverse Engineering Technology: Extraction of Contour Curves

We imported hip images from CVH datasets into AutoCAD (Fig. 1) and designed smooth closed contour curves. The acetabulum side included acetabular bone, cartilage, and labrum, while the femoral bone side included proximal end of the femur and cartilage (Fig. 2). We enlarged the images four times of their original size, drew contour lines

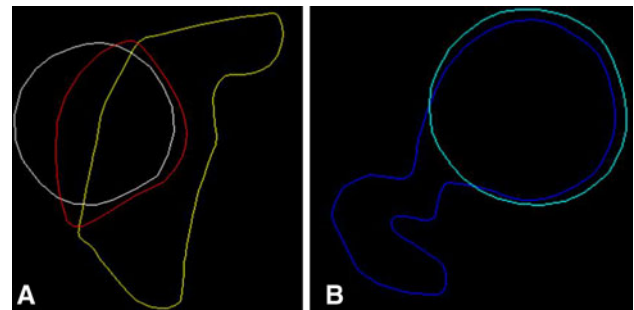


Fig. 2 Extraction of image outline curve. **a** The acetabulum curve includes a smooth closed curve of acetabular bone, cartilage, and glenoid labrum. **b** The femur curve includes a smooth closed curve of proximal femur and articular cartilage (Color figure online)

by hand, extracted the curves layer by layer along the Z axis, and saved them as AutoCAD files.

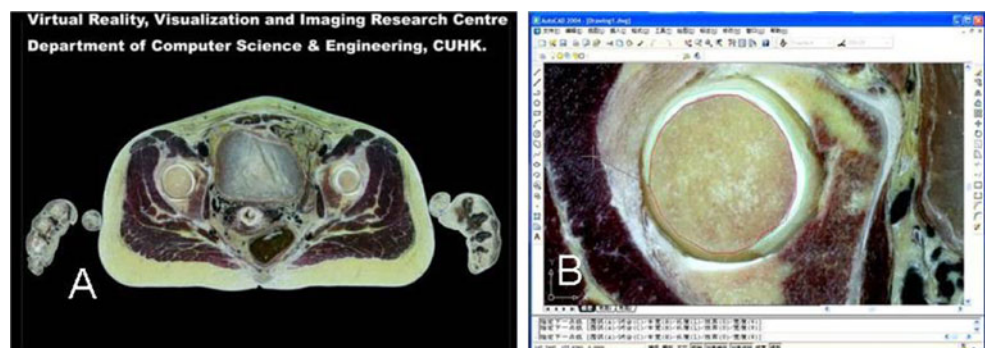
Construction of 3D Models Through Reverse Engineering Technology: Adding Spline Curves

We inserted curves of different colors into one layer of the AutoCAD file. Entities of different colors were constructed separately. The entities with solid colors were formed from the curves in multiple levels in 0.2-mm sections (images of the hip dataset in CHD dataset). The entities with solid colors also contained curves in various colors in their grinding sections. The closed curves of various colors were adjusted by proper spline curves (Figs. 3, 4), which were inserted into the Solidworks software to create an entity.

Construction of 3D Models Through Reverse Engineering Technology: Creation of Smooth Entities

The AutoCAD files described above and containing entity contours were imported into Solidworks; the 3D smooth entity was created as above. The acetabular side was assigned red, yellow, and white entity, while the femoral side was assigned blue and cyan entity (Fig. 5).

Fig. 1 Images of Chinese visible human dataset and Autocad outline. **a** Images of Chinese visible human dataset. **b** Image input into Autocad for outline extraction (Color figure online)



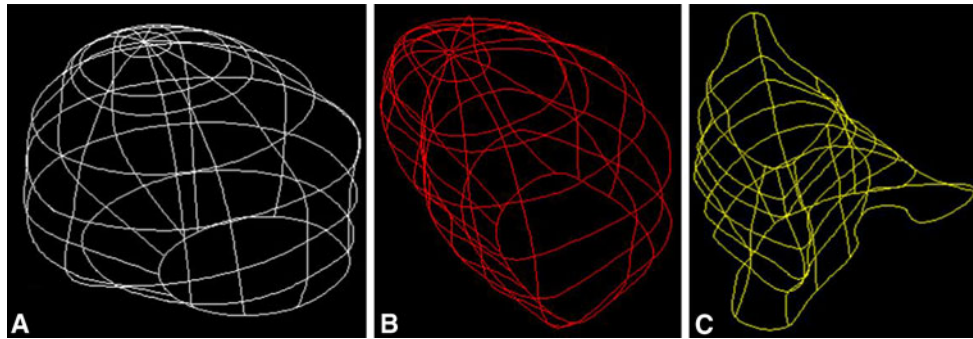


Fig. 3 Addition of the guide curve to the acetabulum. **a** The outline of guide curve is added to the *white curve*. **b** The outline of the guide curve is added to the *red curve*. **c** The outline of the guide curve is added to the *yellow curve* (Color figure online)

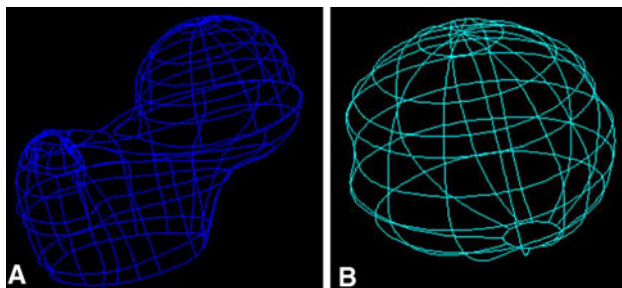


Fig. 4 Addition of the guide curve to the femur. **a** The outline of the guide curve is added to the *blue curve*. **b** The outline of the guide curve is added to the *navy-blue curve* (Color figure online)

Construction of 3D Models Through Reverse Engineering Technology: Creation of Acetabular Bone, Cartilage, and Labrum Entities

All entities and 3D models were constructed by reverse engineering method. The construction of the 3D finite element hip model, which includes the osseous part and cartilage of the acetabulum, glenoid labrum, proximal end of the femoral bone, and femoral cartilage, avoids disadvantages of other construction methods, such as imprecision of cartilage construction and the absence of labrum. Therefore, this method more accurately recapitulates both normal and abnormal conditions in the hip.

The yellow entity contained acetabular bone, while the red entity contained acetabular cartilage and labrum. The labrum and cartilage entities were obtained by separating the yellow entity from the red one; the latter included acetabular cartilage and labrum. The acetabular bone entity was also obtained by removing the yellow entity from the red one. The femoral cartilage entity was obtained by removing the blue entity, which contained the proximal end of the femoral bone, from the cyan one.

Separation of the white entity from the red one yielded the entity that contained acetabular cartilage and glenoid labrum. Then, the yellow entity was separated to yield the glenoid labrum entity. The overlap between this and the

yellow entity was used to obtain the entity which included acetabular cartilage. The acetabular bone entity was obtained by removing yellow entity from the red one. The blue entity that contained the proximal end of the femoral bone was separated from the cyan one. This procedure yielded the femoral cartilage entity.

Construction of 3D Finite Element Model: Assembly of Entities and Material Property Setting

The obtained entities included acetabular bone, cartilage, labrum, proximal end of the femoral bone, and femoral cartilage. These were entered into ABAQUS software as building blocks. The proximal end of the femur was flexed at an angle of 5° and externally rotated at 20° relative to acetabulum. Linear isotropic elastic materials were assigned for acetabular cartilage and labrum. Specifically, elastic moduli of 11.85 and 20 Mpa and Poisson's ratio of 0.45 and 0.4 were used, respectively, for cartilage and labrum [12]. A rigid material was assigned for subchondral bone of acetabulum and the femoral head.

Construction of 3D Finite Element Model: Mesh Generation and Boundary Setting

Revised C3D10M elements were applied to cartilage and labrum with an element size of 1.2 mm. The mesh in the areas of top acetabular cartilage and labrum was refined. The acetabular bone was fixed. Free mesh of tetrahedron approach was adopted for the zone of femoral bone with element size of 2 mm.

Construction of 3D Finite Element Model: Contact Property and Model Verification

A contact property was defined as nonlinear frictional contact, and a penalty method was applied with a frictional coefficient of 0.001 in the friction formula. The external load was applied through the centroid of the femoral head; the pelvis was

considered fixed, while the femoral head was assumed movable in six degrees of freedom. The peak force of a single leg standing (1,358 N; force directions: 7° in frontal plane; -28° in transverse plane), described by Bergmann et al. [13], was loaded to observe the contact area and pressure distribution in the cartilage and labrum of the hip.

Results

Construction of the 3D Entity Model

Extracted contour curves are shown in Figs. 1 and 2, guide curves in Figs. 3 and 4, smooth entities in Fig. 5, and the expected entities of acetabular bone, cartilage, and labrum constructed by removing different parts from various entities are demonstrated in Fig. 6. Figures 1, 2, 3, 4, and 5 represent reverse engineering which was adopted for the process of entity construction. As illustrated in Fig. 6, the entities of acetabular bone, cartilage, and labrum matched the anatomical structure of the human hip. Further different contact surfaces between various entities are shown, achieving an accurate assembly in ABAQUS without any gaps or overlaps which could affect the analysis of contact pressure.

Creation of 3D Finite Element Models

The entities of acetabular bone, cartilage, and labrum were assembled and meshed, and then 3D finite element models

were created. The contact pressure distribution during the loading test in the contact area between acetabular cartilage and labrum is shown in Fig. 7. The contact pressure for cartilage of acetabulum and femoral head mainly occurs in the central areas of the acetabulum and top areas of femoral head during the single or double leg standings. The maximum pressure is 4.94 MPa in acetabulum and 4.77 MPa in femoral head during the single leg standing, which is close to the results of studies adopting traditional approaches [4]. In our study, labrum was taken as an independent element in contact pressure analysis.

Discussion

The unique anatomic structure and complex physiologic functions of the human hip impede biomechanical research in this field. Previously, the articular contact surface area of the hip and pressure distribution were calculated using the stain method or pressure-sensitive film [3]. Rushfeldt et al. [4] implanted prosthetic sensor-equipped femoral head into cadavers and measured stress distribution in the human acetabular cartilage. Further, Brown and Shaw [5] calculated stress distribution in the femoral head and acetabular cartilage using transducers placed in the femoral head cartilage. Hodge et al. [6] implanted prosthetic telemeter-equipped femoral head into natural acetabular cartilage and acquired data of stress distribution in the acetabular cartilage for 1–5 years after surgery. However, despite

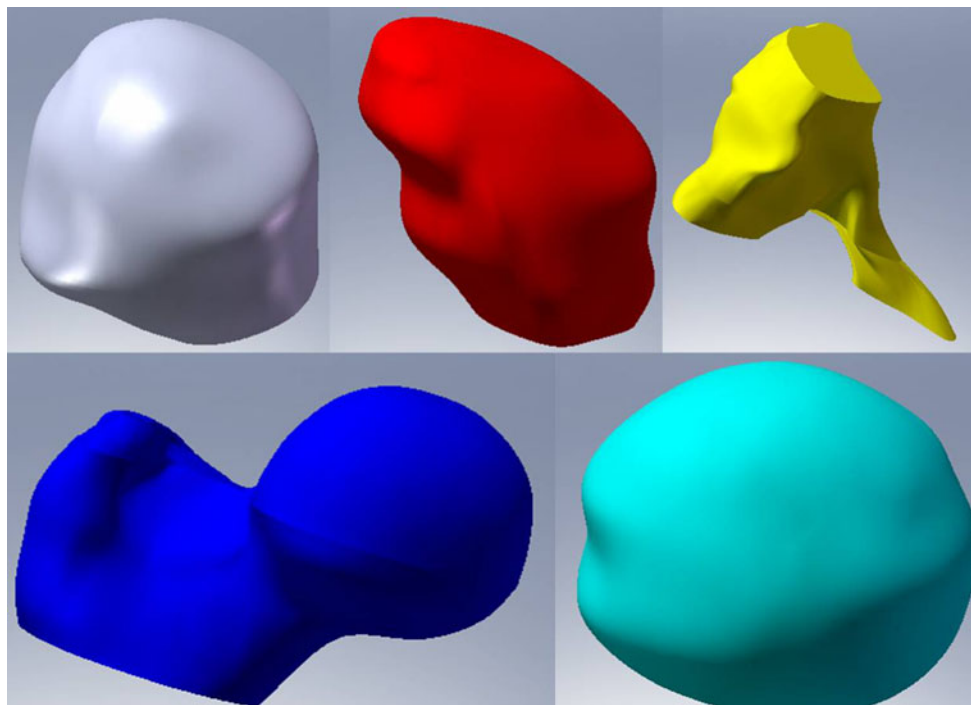


Fig. 5 Different smooth three-dimensional solid substances constructed by Solidworks (Color figure online)

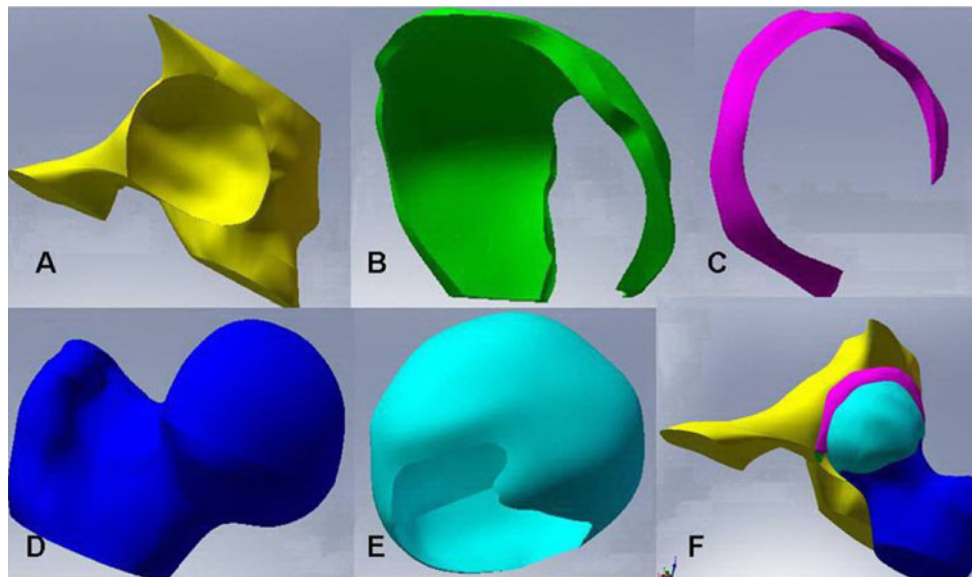


Fig. 6 Compound solid substances after reduction of other smooth solid substances. **a** Solid substance of the acetabulum. **b** Solid substance of the acetabular cartilage. **c** Solid substance of the glenoid

labrum. **d** Osseous solid substance of the femur head. **e** Solid substance of femur head cartilage. **f** Integrated structure of the acetabulum (Color figure online)

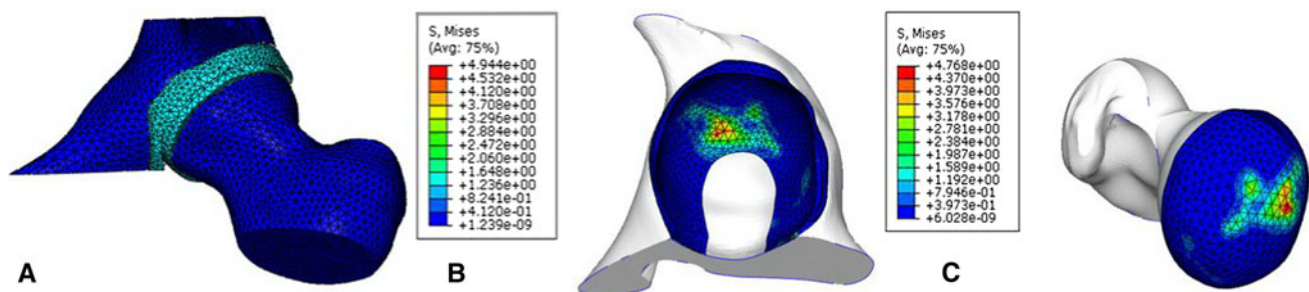


Fig. 7 The three-dimensional (3D) model and verification of the model. **a** The grid of the 3D finite element stress analysis model. **b** Pressure distribution in the contact surface of the acetabular

cartilage. **c** Pressure distribution in the contact surface of the femur head cartilage (Color figure online)

substantial knowledge advances in this field, there are still many problems with such assessments, making it hard to use the data as reference.

Previous studies postulated that acetabular labrum only seals the hip joint (synovial joint) [10]. Konrath et al. [10] indicated that removal of the acetabular labrum does not significantly influence pressure distribution in acetabular cartilage. Still, there are no reports on stress distribution in acetabular cartilage when the hip joint is involved in different activities.

The finite element method is useful for high-fidelity simulation and accurate analysis of complex structures of human organs. It is a biomedical engineering approach based on basic mechanical principles and material science, and utilizes mechanical models and performs biomechanical analysis using computer and specialized software. It has been most commonly used for mechanical digital analyses. In a finite element model, intricate geometric

figures can be simulated by utilizing series of simple meshes with appropriate material features.

Using this model, the contact pressure between components of each model under mechanical load can be calculated. The contact pressure on the surface and the joint are calculated by exact model construction and proper motion simulation [9].

Although the finite element method is capable of achieving a high-fidelity simulation and accurate analysis, previous studies [9] indicated that realistic construction of entity and precise property settings are the pre-requisites for correct results. We could hardly find accurate and clear images of acetabular cartilage and labrum through MRI or double source CT imaging.

As before, some simple tissues and structural models can be built through MRI or double source CT imaging. However, such technology cannot be applied to obtain the contour of cartilage in the hip model construction due to

the complex structure of the hip. Hence, high-fidelity simulation cannot be carried out. In this study, CVH dataset (Third Military Medical University) was utilized to facilitate precise definition of the tissue contour and building a simulation model.

Therefore, we were not able to directly apply these images for constructing 3D finite element hip models. Instead, we often utilized 2D images (e.g., CT images) of bone structure of the hip joint to reconstruct the 3D entity of the bone. The cartilage entity was constructed by setting a layer of cartilage tissue covering the acetabular surface. A glenoid labrum with physiological functions had never been previously analyzed as a single entity in a three-dimensional finite element model. Additionally, the traditional entity cutting construction method cannot be applied to constructing small structures like labrum owing to the low resolution of images, the elaborate procedures, and an enormous amount of work involved.

With the high-resolution hip cutting images from the CVH datasets, smooth entities of relevant parts could be created by extracting the contour curves. By subtracting entities from other entities, we constructed 3D entity models of acetabular bone, cartilage, and labrum; and models of femoral head and cartilage. The entities achieved accurate assembly in ABAQUS without any clearance or overlapping. The above construction process has proved that the model could exactly create entities of acetabular labrum, cartilage, and bone. Moreover, the 3D finite element models are ready for assembly, which makes the meshing process go on well. The process met the requirement of the construction of three-dimensional finite element model.

The traverse images from CVH datasets, comprising complete fine structures of hip joint, could be employed to construct a 3D finite element model of acetabular bone, cartilage, and labrum. The mechanical analysis using the hip finite element model yielded a result close to what is achieved by traditional studies but without their limitations, such as lack of reproducibility, the need of implants, or difficulty in generalization. Even though the level of contact stress is much lower in the labrum, than at the top of acetabular cartilage, the pressure still exists in contact areas.

In conclusion, our study demonstrated that the described model is capable of accurate creation of the cartilage, with construction of labrum as an independent entity, to overcome limitations of previous studies in which the cartilage was artificially added and no labrum was constructed.

Acknowledgments This work was supported by the Research Innovation Fund of the Third Military Medical University (Grant Number 2009XQN24).

Conflict of interest The authors declare no competing interests.

References

1. Macirowski, T., Tepic, S., & Mann, R. W. (1994). Cartilage stresses in the human hip joint. *Journal of Biomechanical Engineering*, *116*, 10–18.
2. von Eisenhart, R., Adam, C., Steinlechner, M., Muller-Gerbl, M., & Eckstein, F. (1999). Quantitative determination of joint incongruity and pressure distribution during simulated gait and cartilage thickness in the human hip joint. *Journal of Orthopaedic Research*, *17*, 532–539.
3. Greenwald, A. S., & O'Connor, J. J. (1971). The transmission of load through the human hip joint. *Journal of Biomechanics*, *4*, 507–528.
4. Rushfeldt, P. D., Mann, R. W., & Harris, W. H. (1981). Improved techniques for measuring in vitro the geometry and pressure distribution in the human acetabulum. II Instrumented endoprosthesis measurement of articular surface pressure distribution. *Journal of Biomechanics*, *14*, 315–323.
5. Brown, T. D., & Shaw, D. T. (1983). In vitro contact stress distributions in the natural human hip. *Journal of Biomechanics*, *16*, 373–384.
6. Hodge, W. A., Fijan, R. S., Carlson, K. L., Burgess, R. G., Harris, W. H., & Mann, R. W. (1986). Contact pressures in the human hip joint measured in vivo. *Proceedings of the National Academy of Sciences of the United States of America*, *83*, 2879–2883.
7. Genda, E., Iwasaki, N., Li, G., MacWilliams, B. A., Barrance, P. J., & Chao, E. Y. (2001). Normal hip joint contact pressure distribution in single-leg standing—Effect of gender and anatomic parameters. *Journal of Biomechanics*, *34*, 895–905.
8. Mavcic, B., Pompe, B., Antolic, V., Daniel, M., Iglic, A., & Kralj-Iglic, V. (2002). Mathematical estimation of stress distribution in normal and dysplastic human hips. *Journal of Orthopaedic Research*, *20*, 1025–1030.
9. Anderson, A. E., Ellis, B. J., Maas, S. A., Peters, C. L., & Weiss, J. A. (2008). Validation of finite element predictions of cartilage contact pressure in the human hip joint. *Journal of Biomechanical Engineering*, *130*, 051008.
10. Konrath, G. A., Hamel, A. J., Olson, S. A., Bay, B., & Sharkey, N. A. (1998). The role of the acetabular labrum and the transverse acetabular ligament in load transmission in the hip. *Journal of Bone and Joint Surgery. American Volume*, *80*, 1781–1788.
11. Zhang, S. X., Liu, Z. J., Tan, L. W., Qiu, M. G., Li, Q. Y., Li, K., et al. (2003). The third report on the Chinese visible human (CVH) datasets. *Journal of Third Military Medical University*, *23*, 1332–1335.
12. Ferguson, S. J., Bryant, J. T., & Ito, K. (2001). The material properties of the bovine acetabular labrum. *Journal of Orthopaedic Research*, *19*, 887–896.
13. Bergmann, G., Deuretzbacher, G., Heller, M., Graichen, F., Rohlmann, A., Strauss, J., et al. (2001). Hip contact forces and gait patterns from routine activities. *Journal of Biomechanics*, *34*, 859–871.